Journal of Superconductivity and Novel Magnetism

Supercurrent generation by spin-twisting itinerant motion of electrons: re-derivation of the ac Josephson effect including the current flow through the leads connected to Josephson junction

--Manuscript Draft--

Manuscript Number:	
Full Title:	Supercurrent generation by spin-twisting itinerant motion of electrons: re-derivation of the ac Josephson effect including the current flow through the leads connected to Josephson junction
Article Type:	Original Research
Keywords:	New Supercurrent Generation mechanism; Spin-vortex; Spin-vortex-induced loop current; Josephson effect
Corresponding Author:	Hiroyasu Koizumi, Ph.D University of Tsukuba Tsukuba, JAPAN
Corresponding Author Secondary Information:	
Corresponding Author's Institution:	University of Tsukuba
Corresponding Author's Secondary Institution:	
First Author:	Hiroyasu Koizumi, Ph.D
First Author Secondary Information:	
Order of Authors:	Hiroyasu Koizumi, Ph.D
	Masashi Tachiki, PhD
Order of Authors Secondary Information:	

Supercurrent generation by spin-twisting itinerant motion of electrons: re-derivation of the ac Josephson effect including the current flow through the leads connected to Josephson junction

Hiroyasu Koizumi

Division of Materials Science, University of Tsukuba, Tsukuba, Ibaraki 305-8573, Japan

Masashi Tachiki

Department of Physics, Tohoku University, Sendai, Miyagi 980-8578, Japan

(Dated: September 19, 2014)

Abstract

Based on a new supercurrent generation mechanism proposed for the cuprate superconductivity [1–4], we re-derive the ac Josephson effect including the current flow through the leads connected to the Josephson junction and the impressed electromotive force. It is noted that the actual experimental boundary condition where the Josephson frequency $2eV_0/h$ (h is Planck's constant, e is the absolute value of electron charge, and V_0 is the dc voltage across the Josephson junction) is measured is different from the one assumed by Josephson, and $2eV_0/h$ is obtained by the electron tunneling instead of the Cooper pair tunneling. It is also indicated that the standard textbook description for the Josephson relation, "if a dc voltage V_0 is applied, the time-variation of ϕ occurs" [5–8] (ϕ is related to the tunneling current as $J_s = J_c \sin\phi$) should be rephrased, " if the time-variation of ϕ is introduced, a voltage difference V_0 appears".

We show that by adding the Rashba spin-orbit interaction to the BCS Hamiltonian, the spin-twisting itinerant motion of electrons is stabilized in the BCS superconductors; thus, it is suggested that the present new supercurrent generation mechanism is also relevant to the BCS superconductors, i.e., the true origin of the supercurrent generation in the BCS superconductors may also be the spin-twisting itinerant motion of electrons.

PACS numbers:

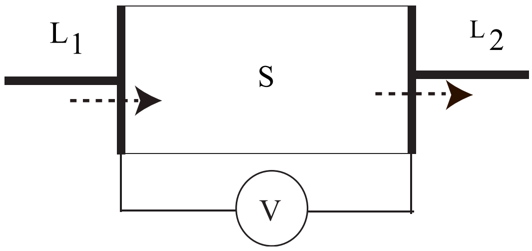

FIG. 1: Schematic set-up of the Kamerlingh Onnes's experiment. A specimen of mercury, S, is connected to leads, L_1 and L_2, and the voltage drop is measured by feeding a current through the leads.

I. INTRODUCTION

In 1911, Kamerlingh Onnes discovered the phase transition in mercury to a state that exhibits electric current flow without a voltage drop (Fig. 1) [9, 10]. This state is called the superconducting state, and has been a focus of attention in physics and materials science since then. A successful microscopic theory for this phase transition was put forward by Bardeen, Cooper and Schrieffer (BCS) [11]. The BCS theory explained the superconducting phase transition as due to the energy gap creation by the Cooper pair formation. The superconducting transition temperature T_c can be calculated as the temperature where the energy gap by the Cooper pair formation is created.

In 1986 a novel high temperature superconductivity was discovery in the cuprate [12]. The superconducting phenomenon in this family of materials is markedly different from the BCS one [11]. Most notably, the superconducting transition temperature T_c is not determined by the energy gap formation by the electron pairing, but it appears to correspond to the temperature where the supercurrent vortices of the coherence length are stabilized [13], suggesting that the cuprate belongs to a different class of superconductors in which the coherence-sized supercurrent loop plays a central role.

Recently, a theory for the cuprate superconductivity in which the coherence-sized persistent loop current is the protagonist of superconductivity was developed [1–4]. For the generation of the persistent loop current, the fact established in the dynamical Jahn-Teller problem was used: when a wave function is multi-component, the twisting of the basis of the components creates a persistent circular motion in the ground state due to the *single-valued requirement of the wave function* [14]. The single-valued requirement of the wave function is one of the postulates Schrödinger imposed to evaluate hydrogen atomic spectrum, and explained the stability of the atom [15]. The solution of the dynamical Jahn-Teller problem indicates that if the same postulate is applied to the multi-component wave function problem, a zero point circular motion becomes possible. This zero point circular motion may be regarded as the consequence of the appearance of a 'fictitious magnetic field' from the Berry phase due to the existence of a singularity in the multi-component wave function [16, 17], but its true physical meaning is the forced whole system motion generated by the single-valued requirement of the total wave function.

If we take the spin degree-of-freedom as the source of the multi-component wave function, the supercurrent is generated by the forced whole system motion induced by the spin-twisting itinerant motion of electrons. The resulting loop current is called, the "spin-vortex-induced loop current (SVILC)" [1–4]. A theory was put forward in which a macroscopic persistent current is generated as a collection of SVILCs and a method was developed to calculate this superconducting wave function [3, 4].

The superconducting wave function in the new theory is given in the following form

$$\Psi(\mathbf{r}^{(1)}, \cdots, \mathbf{r}^{(N)}) = \Psi_0(\mathbf{r}^{(1)}, \cdots, \mathbf{r}^{(N)}) e^{-\frac{i}{2}\sum_{\alpha=1}^{N} \chi(\mathbf{r}^{(\alpha)})} \tag{1}$$

where $\mathbf{r}^{(j)}$ is the coordinate of the jth electron and N is the total number of electrons. Ψ_0 is a currentless multi-valued wave function, where the multi-valuedness arises from the spin-twisting of the itinerant electrons. The phase factor $e^{-\frac{i}{2}\sum_{\alpha=1}^{N} \chi(\mathbf{r}^{(\alpha)})}$ arises to impose the single-valued requirement of the total wave function [3, 4].

Let us explain the mechanism in which the supercurrent is generated from the spin-twisting itinerant motion of electrons in more detail. In order to make the twisting of the spin direction apparent, we change the basis from $\{c^\dagger_{j\uparrow}|\text{vac}\rangle, c^\dagger_{j\downarrow}|\text{vac}\rangle\}$ to $\{a^\dagger_j|\text{vac}\rangle, |b^\dagger_j|\text{vac}\rangle\}$, where $c^\dagger_{j\sigma}$ denotes the creation operators for the localized state at site j with spin σ, $|\text{vac}\rangle$ is vacuum, and j runs through all lattice sites of the system; the creation operators $a^\dagger_j$ and $b^\dagger_j$ are related to $c^\dagger_{j\sigma}$ by

$$\begin{aligned} a^\dagger_j &= e^{-i\frac{\chi_j}{2}} \left(\cos\frac{\zeta_j}{2} e^{-i\frac{\xi_j}{2}} c^\dagger_{j\downarrow} + \sin\frac{\zeta_j}{2} e^{i\frac{\xi_j}{2}} c^\dagger_{j\uparrow} \right) \\ b^\dagger_j &= e^{-i\frac{\chi_j}{2}} \left(-\sin\frac{\zeta_j}{2} e^{-i\frac{\xi_j}{2}} c^\dagger_{j\downarrow} + \cos\frac{\zeta_j}{2} e^{i\frac{\xi_j}{2}} c^\dagger_{j\uparrow} \right) \end{aligned} \tag{2}$$

where variables ξ_j and ζ_j are the azimuth and polar angles of the spin at the jth site,

$\mathbf{S}_j = (S^x_j, S^y_j, S^z_j)$, where S^x_j, S^y_j, and S^z are expressed using ξ_j and ζ_j as

$$S^x_j = S_j \cos\xi_j \sin\zeta_j; \quad S^y_j = S_j \sin\xi_j \sin\zeta_j; \quad S^z_j = S_j \cos\zeta_j. \tag{3}$$

The single particle wave functions are expressed as

$$|\gamma\rangle = \sum_j \left(D^a_\gamma a^\dagger_j + D^b_\gamma b^\dagger_j \right) |\mathrm{vac}\rangle \tag{4}$$

and the many-electron wave function is constructed as a sum of Slater determinants composed of them. The above wave function (molecular orbital) is differet from the one appears in the conventional molecular orbital theory since the singularities arising from the twisting of the spin-directions are taken into account from the beginning; i.e., $a^\dagger_j$ and $b^\dagger_j$ are singular at the centers of the spin-vortices. The obtained many electron wave function is given in the form of Eq. (1), where the correlation effect is included in Ψ_0. The phase factor $e^{-\frac{i}{2}\sum_{\alpha=1}^{N}\chi(\mathbf{r}^{(\alpha)})}$ arises from $e^{-i\frac{\chi_j}{2}}$ in $a^\dagger_j$ and $b^\dagger_j$ in Eq. (2).

The twisting of the spin direction is detected by the nonzeroness of the winding number of ξ along loop C_ℓ defined by

$$w_\ell[\xi] = \frac{1}{2\pi}\sum_{i=1}^{N_\ell}\left[\xi_{C_\ell(i+1)} - \xi_{C_\ell(i)}\right] = \frac{1}{2\pi}\oint_{C_\ell} \nabla\xi \cdot d\mathbf{r} \tag{5}$$

where C_ℓ is a loop in the x-y plane. N_ℓ is the total number of sites on the loop C_ℓ, and $C_\ell(i)$ is the ith site on it with the periodic condition $C_\ell(N_\ell+1) = C_\ell(1)$. The presence of the spin-vortices means that $w_\ell[\xi]$ is nonzero for some loops.

If the electron wave function is obtained only by the energy minimization, we obtain the phase differences of ξ, such as $\xi_i - \xi_j$ [4]. From these phase differences, we can construct ξ and calculate $w_\ell[\xi]$. If the loop C_ℓ encircles a spin-vortex with the winding number $w_\ell[\xi]$, ξ has a jump of value by $2\pi w_\ell[\xi]$. This phase jump causes a sign change of the phase factor $e^{\pm i\frac{\xi_j}{2}}$ in $|\gamma\rangle$ through $a^\dagger_j$ and $b^\dagger_j$ in Eq. (2) if $w_\ell[\xi]$ is an odd number. This sign change is compensated by $e^{-i\frac{\chi_j}{2}}$ to make $|\gamma\rangle$ single-valued. In other word, since $e^{-\frac{i}{2}\sum_{\alpha=1}^{N}\chi(\mathbf{r}^{(\alpha)})}$ gives rise to a whole system motion, the sign change generates a nontrivial whole system motion.

The single-valued requirement of $|\gamma\rangle$ is achieved by imposing the following constraint

$$w_\ell[\xi] + w_\ell[\chi] = \text{even number for any loop } C_\ell, \tag{6}$$

where $w_\ell[\chi]$ is the winding number of χ for the loop C_ℓ. If the above condition is satisfied, the change of $\pm\xi_j - \chi_j$ after the circular transportation along C_ℓ is a multiple of 4π; then, the sign change is compensated as $e^{\frac{i}{2}(\pm\xi_j-\chi_j)} \to e^{\frac{i}{2}(\pm\xi_j-\chi_j+4\pi w)} = e^{\frac{i}{2}(\pm\xi_j-\chi_j)}$ (w is an integer); consequently, $a_j^\dagger$ and $b_j^\dagger$ become single-valued.

Denoting the energy functional that depends on $\nabla\chi$ as $E[\nabla\chi]$, the constrained minimization is performed to obtain $\nabla\chi$. For this purpose, the method of Lagrange multiplier is used with the following functional

$$F[\nabla\chi] = E[\nabla\chi] + \sum_{\ell=1}^{N_{\rm loop}} \lambda_\ell \left(\oint_{C_\ell} \nabla\chi \cdot d\mathbf{r} - 2\pi\bar{w}_\ell \right), \tag{7}$$

where λ_ℓs are the Lagrange multipliers, $N_{\rm loop}$ is the number of independent loops (i.e., any loops in the system can be constructed from them), and $\bar{w}_\ell$ is a value of $w_\ell[\chi]$ that satisfies the condition in Eq. (6). Different current patters are obtained by different combinations of $\bar{w}_\ell, \ell = 1, \cdots, N_{\rm loop}$. They form metastable states protected by the winding numbers $w_\ell[\chi]$'s.

Including the electromagnetic vector potential $\mathbf{A}^{\rm em}$, the functional $E[\nabla\chi]$ is given by

$$E[\nabla\chi] = \langle\Psi|H[\mathbf{A}^{\rm em}]|\Psi\rangle = \langle\Psi_0|H[\mathbf{A}^{\rm em} - \frac{c\hbar}{2e}\nabla\chi]|\Psi_0\rangle, \tag{8}$$

where $H[\mathbf{A}^{\rm em}]$ is the Hamiltonian of the system. The phase factor $e^{-\frac{i}{2}\sum_{j=1}^{N}\chi(\mathbf{r}^{(j)})}$ is transferred from the wave function to the Hamiltonian in the rightmost expression in Eq. (8).

From the stationary condition $\delta F[\nabla\chi]/\delta\nabla\chi = 0$, the current density is obtained as

$$\mathbf{j} = -c\frac{\delta E[\nabla\chi]}{\delta \mathbf{A}^{\rm em}} = \frac{2e}{\hbar}\frac{\delta E[\nabla\chi]}{\delta\nabla\chi} = -\frac{2e}{\hbar}\sum_{\ell=1}^{N_{\rm loop}} \lambda_\ell \frac{\delta}{\delta\nabla\chi}\oint_{C_\ell} \nabla\chi \cdot d\mathbf{r}. \tag{9}$$

This is the supercurrent density in the new theory which is expressed as a sum of loop currents. The criterion of the current generation around loop C_ℓ is that $\frac{\delta E[\nabla\chi]}{\delta\nabla\chi} \neq 0$ is satisfied for the change of $\nabla\chi$ within the constraint of the winding number $w_\ell[\chi]$; if such loops are connected through a macroscopic region, a macroscopic current is possible.

As seen in Eq. (8), the vector potential $\mathbf{A}^{\rm em}$ always appears as a part of the sum

$$\mathbf{A}^{\rm eff} = \mathbf{A}^{\rm em} - \frac{c\hbar}{2e}\nabla\chi \tag{10}$$

This is gauge invariant due to the fact that $\nabla\chi$ is optimized; when, the vector potential with a different gauge $\mathbf{A}'^{\rm em} = \mathbf{A}'^{\rm em} + \nabla g$ is employed, the optimized $\nabla\chi$ becomes $\nabla\chi' = \nabla\chi + \frac{2e}{c\hbar}\nabla g$; thus, the sum remains the same. We may regard $\mathbf{A}^{\rm eff}$ as the effective vector potential in the superconducting state.

The new theory explains the flux quantum $hc/2e$. In order to see this, we compare the gauge invariant $\mathbf{A}^{\text{eff}}$ with the gauge invariant combination $\mathbf{A}^{\text{em}}+\frac{c\hbar}{2e}\nabla\theta$ appears in the current expression of the Ginzburg-Landau theory

$$\mathbf{j}=-\frac{(2e)^2\rho_s}{2m^*c}\left(\mathbf{A}^{\text{em}}+\frac{c\hbar}{2e}\nabla\theta\right), \tag{11}$$

where m^* is the effective mass of electron and ρ_s is the superconducting carrier density. The macroscopic wave function for the Ginzburg-Landau equation is expressed as $\Psi_{GL}=\rho_s^{1/2}e^{i\theta}$. The comparison leads to the identification $\chi=-\theta$. In the new theory, it is shown that the macroscopic wave function for the phenomenological Ginzburg-Landau equation is given by $(\rho_e/2)^{1/2}e^{-i\chi}$ where ρ_e is the electron density given by $\rho_e=2\rho_s$ [4]. Then, the flux quantum is obtained as $\Phi_0=hc/2e$ [4].

In the following, we re-derive the ac Josephson effect using the new theory described above. A similar argument was already given in [1]. However, the present re-derivation is a significantly improved one due to the development of the theory afterward; it is much more elaborated by including the current flow through the leads connected to the Josephson junction and the impressed electromotive force in the Hamiltonian. In the course of re-derivation, it is noted that the boundary condition for the actual measurement of the ac Josephson effect is different from the one assumed by Josephson for the prediction. We also consider the possible application of the new supercurrent generation mechanism to the BCS superconductors. It is shown that the new theory is applicable if the Rashba spin-orbit interaction [18] is add to the BCS theory.

II. RE-DERIVATION OF THE AC JOSEPHSON EFFECT INCLUDING THE CURRENT FLOW FROM THE LEADS

First, we note that the relation in Eq. (10) means that the time-component partner of $\mathbf{A}^{\text{eff}}$,

$$\varphi^{\text{eff}}=\varphi^{\text{em}}+\frac{\hbar}{2e}\dot{\chi} \tag{12}$$

is also gauge invariant, where φ^{em} is the electromagnetic scalar potential. We regard φ^{eff} as the effective scalar potential in the superconducting state, and relate it to the chemical potential μ as $\mu=-e\varphi^{\text{eff}}$.

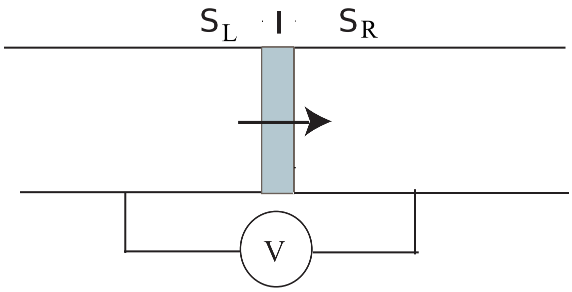

FIG. 2: Schematic set-up of the Josephson junction for which Josephson assumed in the predictions. 'S$_L$' and 'S$_R$' indicate the superconductor parts of the junction. The weak link is denoted as 'I' .

Let us state the Josephson's prediction. He predicted that the current given by

$$J_s = J_c \sin\phi, \tag{13}$$

would flow through the junction made of two superconductors coupled by a weak link as a consequence of the Cooper pair tunneling, where J_c is the critical current and ϕ is the difference of the phase of the macroscopic wave function for superconductivity [19, 20].

Further, he predicted that if a dc voltage V_0 exists across the weak link, ϕ would show the time-dependence

$$\frac{d\phi}{dt} = \frac{2eV_0}{\hbar}, \tag{14}$$

thus, an ac current of amplitude J_c and the frequency

$$\nu_{\mathrm{J}} = 2eV_0/h \tag{15}$$

would be generated [19]. Josephson employed the barrier tunneling formalism [21] and considered the electron-pair tunneling between the two superconductors for his prediction; thus, the situation assumed by him is the one depicted in Fig. 2.

On the other hand, in the actual experimental situation where Josephson frequency is measured, a dc current is fed through the leads connected to the junction as shown in Fig. 3. The tunneling current is measured with the concurrent supercurrent flow in the superconductor parts of the junction, where each superconductor part plays the similar role as the specimen in Fig. 1. The weak link acts as a coupler between such two dc current flowing superconductors.

Now we shall calculate the current through the junction by employing the actual experimental boundary condition. We consider a simplified model in which the current feeding

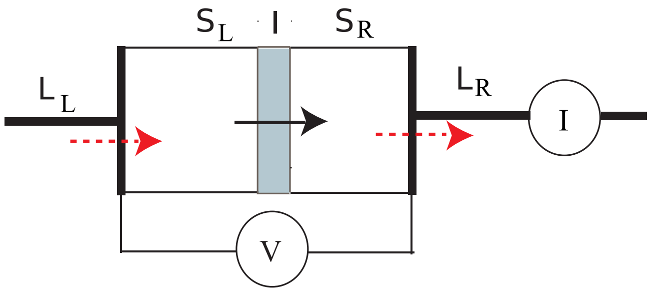

FIG. 3: Schematic set-up of the Josephson junction for which experimental measurements are actually performed. The dc current is fed from the lead connected to the junction, thus, the dc current exists in the superconductors S_L and S_R.

from the leads is taken into account by adding an external path that connects the two superconductors as shown in Fig. 4. The external path contains the part that generates the impressed electromotive force.

The Hamiltonian for this model is expressed as

$$\hat{H} = \hat{K}_{\rm Link} + \hat{K}_{\rm Ex} + \hat{H}_{\rm Super}. \tag{16}$$

$\hat{H}_{\rm Super}$ is the Hamiltonian for the two superconductors in the junction; it yields the solution that describes the dc currents through them with the time-independent optimized $\nabla\chi$. This $\nabla\chi$ ensures the current flow through each superconductors without a voltage drop.

$\hat{K}_{\rm Link}$ denotes the hopping term between the two superconductors through the weak link given by

$$\begin{aligned}\hat{K}_{\rm Link} &= -\sum_{k\in S_L, j\in S_R,\sigma} T^{\rm Link}_{kj} \exp\left(-i\frac{e}{\hbar c}\int_j^k \mathbf{A}^{\rm em}\cdot d\mathbf{r}\right) c^\dagger_{k\sigma} c_{j\sigma} + {\rm h.c.} \\ &= -\sum_{k\in S_L, j\in S_R} T^{\rm Link}_{kj} \exp\left(-i\frac{e}{\hbar c}\int_j^k \mathbf{A}^{\rm em}\cdot d\mathbf{r} + i\frac{\chi_k+\chi_L-\chi_j-\chi_R}{2}\right) \\ &\times \left[\cos\frac{\xi_k-\xi_j}{2}(a^\dagger_k a_j + b^\dagger_k b_j) - i\sin\frac{\xi_k-\xi_j}{2}(a^\dagger_k b_j + b^\dagger_k a_j)\right] + {\rm h.c.}\end{aligned} \tag{17}$$

where $k\in S_L$ and $j\in S_R$ denote the lattice points in the left and right superconductors, respectively. In order to make the presence of χ apparent, we employ creation operators, $a^\dagger_j$ and $b^\dagger_j$, and annihilation operators, a_j and b_j. $T^{\rm Link}_{kj}$ is non-zero for k and j that are located in the edges of the superconductors contacted with the weak link. χ_L and χ_R are time-

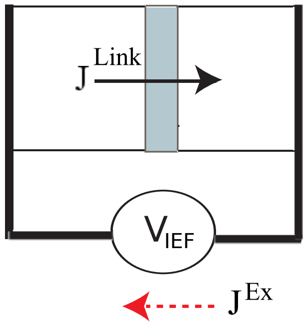

FIG. 4: Schematic set-up we consider for the Hamiltonian in Eq. (16). $V_{\rm IEF}$ denotes the voltage produced by the impressed electromotive force. A dc supercurrent flows through each superconductor in the junction as in the specimen in the Onnes's experiment depicted in Fig. 1.

dependent part of χ in the left and right superconductors, respectively; χ_j and χ_k describe the dc current flow in the two superconductors, and are time-independent.

$\hat{K}_{\rm Ex}$ is the term for the current feeding through the leads connected to the junction; it also contains the impressed electromotive force through the vector and scalar potentials $\mathbf{A}^{\rm Ex}$ and $\varphi^{\rm Ex}$; they are not the real potentials but describe the impressed electromotive force through the "electric field" $\mathbf{E}^{\rm Ex}$ given by

$$\mathbf{E}^{\rm Ex} = -\nabla\varphi^{\rm Ex} - \frac{1}{c}\frac{\partial}{\partial t}\mathbf{A}^{\rm Ex}. \tag{18}$$

The expression for $\hat{K}_{\rm Ex}$ is

$$\begin{aligned}\hat{K}_{\rm Ex} &= -\sum_{k\in S_R, j\in S_L} T^{\rm Ex}_{kj} \exp\left(-i\frac{e}{\hbar c}\int_j^k \mathbf{A}^{\rm Ex}\cdot d\mathbf{r} + i\frac{\chi_k+\chi_R-\chi_j-\chi_L}{2}\right) \\ &\times \left[\cos\frac{\xi_k-\xi_j}{2}(a^\dagger_k a_j + b^\dagger_k b_j) - i\sin\frac{\xi_k-\xi_j}{2}(a^\dagger_k b_j + b^\dagger_k a_j)\right] + \text{h.c.}\end{aligned} \tag{19}$$

where $T^{\rm Ex}_{kj}$ is non-zero for k and j that are located in the edges of the superconductors connected to the leads. The integration is done along the external path.

The current through the weak link is expressed as

$$J^{\rm Link} = \sum_{k\in S_L, j\in S_R} J^{\rm Link}_{kj} \sin\left(\frac{e}{\hbar c}\int_j^k \mathbf{A}^{\rm em}\cdot d\mathbf{r} + \frac{\chi_R+\chi_j-\chi_L-\chi_k}{2} - \alpha_{kj}\right) \tag{20}$$

where $J^{\rm Link}_{kj} = -2eT^{\rm Link}_{kj}A_{kj}/\hbar$ with A_{kj} and α_{kj} defined through

$$A_{kj}e^{i\alpha_{kj}} = \left\langle \cos\frac{\xi_k-\xi_j}{2}(a^\dagger_k a_j + b^\dagger_k b_j) - i\sin\frac{\xi_k-\xi_j}{2}(a^\dagger_k b_j + b^\dagger_k a_j)\right\rangle. \tag{21}$$

Similarly, the current through the external path is expressed as

$$J^{\mathrm{Ex}} = \sum_{k \in S_R, j \in S_L} J_{kj}^{\mathrm{Ex}} \sin\left(\frac{e}{\hbar c} \int_j^k \mathbf{A}^{\mathrm{Ex}} \cdot d\mathbf{r} + \frac{\chi_L + \chi_j - \chi_R - \chi_k}{2} - \alpha_{kj} \right) \tag{22}$$

where $J_{kj}^{\mathrm{Ex}} = -2eT_{kj}^{\mathrm{Ex}} A_{kj}/\hbar$.

In the experiment, a dc current is fed. Thus, the phase in J^{Ex} is time-independent, yielding

$$0 = \frac{e}{\hbar c} \int_j^k \frac{\partial}{\partial t} \mathbf{A}^{\mathrm{Ex}} \cdot d\mathbf{r} + \frac{\dot{\chi}_L - \dot{\chi}_R}{2} = \frac{e}{\hbar c} \int_L^R \frac{\partial}{\partial t} \mathbf{A}^{\mathrm{Ex}} \cdot d\mathbf{r} + \frac{\dot{\chi}_L - \dot{\chi}_R}{2}, \tag{23}$$

where $j \in S_L$ and $k \in S_R$ are replaced by common values L and R, respectively.

From Eq. (12) we have

$$-e\varphi_L^{\mathrm{eff}} = -e\varphi_L^{\mathrm{em}} - \frac{\hbar}{2} \dot{\chi}_L; \quad -e\varphi_R^{\mathrm{eff}} = -e\varphi_R^{\mathrm{em}} - \frac{\hbar}{2} \dot{\chi}_R \tag{24}$$

We identify the gauge invariant quantities $-e\varphi_L^{\mathrm{eff}}$ and $-e\varphi_R^{\mathrm{eff}}$ as the chemical potentials μ_L in S_L, and μ_R in S_R, respectively. Then, the relation in Eq. (23) becomes

$$0 = -\frac{e}{\hbar} \int_L^R \mathbf{E}^{\mathrm{Ex}} \cdot d\mathbf{r} - \frac{\mu_L - \mu_R}{\hbar}, \tag{25}$$

which means that the impressed electromotive force gives rise to the chemical potential difference $\mu_L - \mu_R$.

The time-derivative of the phase of J^{Link} is calculated as

$$\begin{aligned} \dot{\phi}_{kj}^{\mathrm{Link}} &= \frac{e}{\hbar c} \int_j^k \frac{\partial}{\partial t} \mathbf{A}^{\mathrm{em}} \cdot d\mathbf{r} + \frac{\dot{\chi}_R - \dot{\chi}_L}{2} = \frac{e}{\hbar c} \int_R^L \frac{\partial}{\partial t} \mathbf{A}^{\mathrm{em}} \cdot d\mathbf{r} + \frac{\dot{\chi}_R - \dot{\chi}_L}{2} \\ &= -\frac{e}{\hbar} \int_R^L \mathbf{E}^{\mathrm{em}} \cdot d\mathbf{r} - \frac{\mu_R - \mu_L}{\hbar} \end{aligned} \tag{26}$$

where the electric field in the weak link $\mathbf{E}^{\mathrm{em}}$ is given by

$$\mathbf{E}^{\mathrm{em}} = -\nabla \varphi^{\mathrm{em}} - \frac{1}{c} \frac{\partial}{\partial t} \mathbf{A}^{\mathrm{em}}. \tag{27}$$

We denote the voltage across the junction by V;

$$\int_L^R \mathbf{E}^{\mathrm{em}} \cdot d\mathbf{r} = V \tag{28}$$

The above voltage should be equal to the voltage generated by the impressed electromotive force. Thus, we have

$$\int_L^R \mathbf{E}^{\mathrm{Ex}} \cdot d\mathbf{r} = -V, \tag{29}$$

which yields,

$$eV = \mu_L - \mu_R \tag{30}$$

from Eq. (25).

Then, $\dot{\phi}_{kj}^{\rm Link}$ becomes

$$\dot{\phi}_{kj}^{\rm Link} = \frac{2eV}{\hbar} \tag{31}$$

This corresponds the Josephson relation give in Eq. (14) with $V = V_0$.

Since $J^{\rm Ex}$ is a dc current, $J^{\rm Link}$ must be also a dc current in the quasi-stationary condition. One way to achieve this is to put $\dot{\phi}_{kj}^{\rm Link} = 0$, i.e., $V = 0$. This yields,

$$J_{dc}^{\rm Link} = \sum_{k \in S_L, j \in S_R} J_{kj}^{\rm Link} \sin \phi_{kj}^0 \tag{32}$$

where ϕ_{kj}^0 is constant. This describes the dc Josephson effect [22].

It is known that there is an another way to have a dc current [23, 24]. It is achieved by choosing

$$\phi_{kj}^{\rm Link} = -\frac{2eV_0}{\hbar} t + \frac{2eV_1}{\hbar\omega} \sin \omega t + \phi^0 \tag{33}$$

for all pairs of (k, j) that satisfy $J_{kj}^{\rm Link} \neq 0$.

Then, $J^{\rm Link}$ is given by

$$\begin{aligned} J_{ac}^{\rm Link} &= \sin\left(-\frac{2eV_0}{\hbar} t + \frac{2eV_1}{\hbar\omega} \sin \omega t + \phi^0 \right) \sum_{k \in S_L, j \in S_R} J_{kj}^{\rm Link} \\ &= J_c \sum_{n=-\infty}^{\infty} J_n\left(\frac{2eV_1}{\hbar\omega} \right) \sin\left(n\omega t - \frac{2eV_0}{\hbar} t + \phi^0 \right) \end{aligned} \tag{34}$$

where $J_c = \sum_{k \in S_L, j \in S_R} J_{kj}^{\rm Link}$, and the identity $e^{iz \sin\theta} = \sum_{n=-\infty}^{\infty} J_n(z) e^{in\theta}$ is used.

The above current expression indicates that if the condition

$$n\omega = \frac{2eV_0}{\hbar} \tag{35}$$

is satisfied, a quasi-stationary current flows. This explains that Josephson frequency $\frac{2eV_0}{h}$ observed in the 'inverse ac Josephson effect', where an oscillation field is supplied, externally, or a spontaneous appearance of the oscillating field occurs due to the electromagnetic wave emission [23, 24]. Note that 2 in $\frac{2eV_0}{h}$ is a consequence that there are two contributions with the same magnitude in Eq. (26). If the same calculation is done for the Cooper pair tunneling, we obtain $n\omega = \frac{4eV_0}{\hbar}$, which disagrees with the experimental result, indicating that the origin of the Josephson effect is not the Cooper pair tunneling.

The new theory explains the absence of the 'normal ac Josephson effect' ('the ac current generation with amplitude J_c and frequency ν_J by applying the dc voltage V_0') [25–29]. Josephson predicted the occurrence of this effect, however, it has not been observed. In the new theory, the absence is explained as due to the fact that the supercurrent in the superconductors in the junction is always dc.

In standard textbooks, the Josephson relation in Eq. (14) is described that "if a dc voltage V_0 is applied, the time-variation of ϕ" occurs [5–8]. However, the actual experimental result is that " if a time-variation of ϕ is introduced, a voltage difference V_0 appears", which agrees with the present re-derivation.

Characteristic behaviors of the maximum supercurrent through the Josephson junctions in a magnetic field are also explained by the new theory [1]. There are subtle differences between the currently-accepted theory and the new theory; they may be used to check the validity of the new theory.

III. MODIFICATION OF THE PAIRING STATES IN THE BCS SUPERCONDUCTORS BY THE RASHBA SPIN-ORBIT INTERACTION: APPEARANCE OF THE SPIN-TWISTING ITINERANT MOTION OF ELECTRONS

We show in this section that the new supercurrent generation mechanism can be applied to the BCS superconductors if the Rashba spin-orbit interaction [18] is added to the BCS Hamiltonian. By this addition, the pairing states of the Cooper pair are modified to those generate circular itinerant motion with twisting spin direction. Then, the forced whole system motion protected by the topological winding numbers arises as will be shown below.

Let us add the Rashba spin-orbit interaction given by

$$H_{so} = \lambda \mathbf{E}^{\mathrm{em}} \cdot (\boldsymbol{\sigma} \times \hat{\mathbf{p}}) \tag{36}$$

to the BCS theory [18], where λ is the spin-orbit coupling parameter, $\mathbf{E}^{\mathrm{em}}$ is the electric field, $\boldsymbol{\sigma}$ is the vector of Pauli matrices, and $\hat{\mathbf{p}}$ is the momentum operator [18].

We take the electric filed in the z direction $\mathbf{E}^{\rm em} = (0, 0, E_{\rm em})$, and expressed H_{so} as

$$H_{so}^{\rm cyl} = \lambda E_{\rm em} \left[e^{-i\phi} \left(\frac{\partial}{\partial \rho} - \frac{i}{\rho} \frac{\partial}{\partial \phi} \right) |\uparrow\rangle\langle\downarrow| - e^{i\phi} \left(\frac{\partial}{\partial \rho} + \frac{i}{\rho} \frac{\partial}{\partial \phi} \right) |\downarrow\rangle\langle\uparrow| \right], \tag{37}$$

where ρ and ϕ are cylindrical coordinates related to the Cartesian x and y coordinates as $x = \rho \cos\phi$ and $y = \rho \sin\phi$, respectively.

In the BCS ground state the pairing occurs between $(\mathbf{k}, \uparrow)$ and $(-\mathbf{k}, \downarrow)$, and the state vector is given by $\varphi_{\mathbf{k}\sigma} = \frac{1}{\sqrt{\mathcal{V}}} e^{-i\mathbf{k}\cdot\mathbf{r}} |\sigma\rangle$ where $|\sigma\rangle$ is the spin state vector with $\sigma = \uparrow$ or $\downarrow$, $\mathcal{V}$ is the volume of the system, and $\mathbf{r}$ is the spatial coordinate. Using the creation operators $c^\dagger_{\mathbf{k}\sigma}$ for $\varphi_{\mathbf{k}\sigma}$, the BCS state vector is given by

$$|{\rm BCS}\rangle = \prod_{\mathbf{k}} (u_{\mathbf{k}} + v_{\mathbf{k}} c^\dagger_{\mathbf{k}\uparrow} c^\dagger_{-\mathbf{k}\downarrow}) |{\rm vac}\rangle, \tag{38}$$

where $u_{\mathbf{k}}$ and $v_{\mathbf{k}}$ are real variational parameters that satisfy $u_{\mathbf{k}}^2 + v_{\mathbf{k}}^2 = 1$ [11]. This particle number non-fixed state vector facilitates calculations involving the electron pair-correlation that yields an energy gap in single-particle excitations. Since the particle number distribution has a sharp peak at the mean-value N, the obtained wave function can be practically regarded as that for a state with N particles. We regard that the state vector in Eq. (38) is an approximate wave function for N electrons with neglecting the particle number distribution.

In the following, we consider a ring-shaped system of radius R in the x-y plane. The position in this ring is specified by the angle ϕ as $(x, y) = (R\cos\phi, R\sin\phi)$ or the length ℓ defined by $\ell = R\phi$, $(0 \leq \phi < 2\pi)$. The Rashba spin-orbits interaction for electrons in this ring is given by

$$H_{so}^{\rm ring} = -i\lambda E_{\rm em} \left(e^{-i\phi} \frac{d}{d\ell} |\uparrow\rangle\langle\downarrow| + e^{i\phi} \frac{d}{d\ell} |\downarrow\rangle\langle\uparrow| \right). \tag{39}$$

The kinetic energy is given by

$$H_0^{\rm ring} = -\frac{1}{2m^*} \frac{d^2}{d\ell^2}, \tag{40}$$

where m^* is the electron effective mass, where $\hbar$ is taken to be unity.

If we neglect the spin-orbit interaction, the electron pairing will occur between the states $\varphi_{k\uparrow}(\ell)$ and $\varphi_{-k\downarrow}(\ell)$, where $\varphi_{k\sigma}(\ell)$ is given by

$$\varphi_{k\sigma}(\ell) = \frac{e^{ik\ell}}{\sqrt{2\pi R}} |\sigma\rangle. \tag{41}$$

In the presence of the Rashba spin-orbit interaction, we anticipate that electrons will create spin-vortices and loop currents in the manner similar to the spin-vortex superconductivity theory [3, 4]. Then, by ansatz, we consider the pairing of two states, $\varphi^a_k(\ell)$ and $\varphi^b_{-k}(\ell)$, where $\varphi^a_k(\ell)$ and $\varphi^b_k(\ell)$ are given by

$$\begin{aligned}
\varphi^a_k(\ell) &= \frac{e^{ik\ell - i\frac{\chi^a(\ell)}{2}}}{\sqrt{2\pi R}}\left(\cos\frac{\zeta(\ell)}{2}e^{-i\frac{\xi(\ell)}{2}}|\uparrow\rangle + \sin\frac{\zeta(\ell)}{2}e^{i\frac{\xi(\ell)}{2}}|\downarrow\rangle\right) \\
\varphi^b_k(\ell) &= \frac{e^{ik\ell - i\frac{\chi^b(\ell)}{2}}}{\sqrt{2\pi R}}\left(-\sin\frac{\zeta(\ell)}{2}e^{-i\frac{\xi(\ell)}{2}}|\uparrow\rangle + \cos\frac{\zeta(\ell)}{2}e^{i\frac{\xi(\ell)}{2}}|\downarrow\rangle\right).
\end{aligned} \tag{42}$$

Here, χ^a and χ^b are angular variables with period 2π added to make the above wave functions single-valued. The single-valued requirement of the wave function becomes non trivial when ξ changes for the excursion around the ring. We will show below that the $\varphi^a_k(\ell)$ and $\varphi^b_{-k}(\ell)$ pairing is more stable than $\varphi_{k\uparrow}(\ell)$ and $\varphi_{-k\downarrow}(\ell)$ paring if the ring is sufficiently large.

Let us denote the closed path along the ring by C. Then, the winding number of ξ for C is calculated as

$$w_C[\xi] = \frac{1}{2\pi}\oint_C \nabla\xi \cdot d\mathbf{r} = \int_0^{2\pi} \frac{d\xi}{d\phi}d\phi. \tag{43}$$

After the excursion $\phi = 0 \to 2\pi$, ξ becomes $\xi(2\pi R) = \xi(0) + 2\pi w_C[\xi]$. If $w_C[\xi]$ is an odd integer, the phase factors in Eq. (42) change signs as $e^{\pm i\frac{\xi(0)}{2}} \to e^{\pm i\frac{\xi(2\pi R)}{2}} = -e^{\pm i\frac{\xi(0)}{2}}$. The angular variables χ^a and χ^b are added to compensate this sign-change to make $\varphi^a_k(\ell)$ and $\varphi^b_k(\ell)$ single-valued. The condition for the compensation is given by

$$w_C[\xi] + w_C[\chi^a] = \text{even number}; \quad w_C[\xi] + w_C[\chi^b] = \text{even number}. \tag{44}$$

Note that $\varphi^a_k(\ell)$ and $\varphi^b_k(\ell)$ become time-reversal partners if the condition $\chi^a = -\chi^b$ is satisfied.

The spin-density for φ^a_k and φ^b_k are calculated as

$$\begin{aligned}
(\varphi^a_k)^*\hat{s}^x\varphi^a_k &= -(\varphi^b_k)^*\hat{s}^x\varphi^b_k = \frac{1}{4\pi R}\cos\xi\sin\zeta \\
(\varphi^a_k)^*\hat{s}^y\varphi^a_k &= -(\varphi^b_k)^*\hat{s}^y\varphi^b_k = \frac{1}{4\pi R}\sin\xi\sin\zeta \\
(\varphi^a_k)^*\hat{s}^z\varphi^a_k &= -(\varphi^b_k)^*\hat{s}^z\varphi^b_k = \frac{1}{4\pi R}\cos\zeta,
\end{aligned} \tag{45}$$

where the spin operators are defined by

$$\hat{s}^x = \frac{1}{2}\left(|\uparrow\rangle\langle\downarrow| + |\downarrow\rangle\langle\uparrow|\right), \; \hat{s}^y = \frac{i}{2}\left(-|\uparrow\rangle\langle\downarrow| + |\downarrow\rangle\langle\uparrow|\right), \; \hat{s}^z = \frac{1}{2}\left(|\uparrow\rangle\langle\uparrow| - |\downarrow\rangle\langle\downarrow|\right). \tag{46}$$

This indicates that the direction of spin for φ_k^a and that for φ_k^b are mutually opposite. Thus, the total spin-density for the φ_k^a and φ_{-k}^b pair is zero.

The current-densities of φ_k^a and φ_k^b along the ring are calculated as

$$\begin{aligned}(\varphi_k^a)^* \frac{q}{m^* i}\frac{d}{d\ell}\varphi_k^a &= \frac{q}{2\pi m^* R}\left(k - \frac{1}{2}\frac{d\chi^a}{d\ell} - \frac{1}{2}\frac{d\xi}{d\ell}\cos\zeta\right) \\ (\varphi_k^b)^* \frac{q}{m^* i}\frac{d}{d\ell}\varphi_k^b &= \frac{q}{2\pi m^* R}\left(k - \frac{1}{2}\frac{d\chi^b}{d\ell} + \frac{1}{2}\frac{d\xi}{d\ell}\cos\zeta\right),\end{aligned} \tag{47}$$

where q is the charge on the electron $q = -e$.

The current density carried by the φ_k^a and φ_{-k}^b pair is thus given by

$$j_{pair}^{\text{ring}} = -\frac{q}{4\pi m^* R}\frac{d(\chi^a + \chi^b)}{d\ell}, \tag{48}$$

which is zero when$\varphi_k^a(\ell)$ and $\varphi_k^b(\ell)$ become time-reversal partners.

The spin-orbit interaction energy densities of φ_k^a and φ_k^b are calculated as

$$\begin{aligned}(\varphi_k^a)^* H_{so}^{\text{ring}}\varphi_k^a &= \frac{\lambda E_{\text{em}}}{2\pi R}\Big[e^{-i(\phi-\xi)}\left(k - \frac{1}{2}\frac{d\chi^a}{d\ell} + \frac{1}{2}\frac{d\xi}{d\ell}\right)\frac{\sin\zeta}{2} + e^{i(\phi-\xi)}\left(k - \frac{1}{2}\frac{d\chi^a}{d\ell} - \frac{1}{2}\frac{d\xi}{d\ell}\right)\frac{\sin\zeta}{2} \\ &+ \frac{i}{2}\frac{d\zeta}{d\ell}\left(\sin^2\frac{\zeta}{2}e^{i(\phi-\xi)} - \cos^2\frac{\zeta}{2}e^{-i(\phi-\xi)}\right)\Big] \\ (\varphi_k^b)^* H_{so}^{\text{ring}}\varphi_k^b &= -\frac{\lambda E_{\text{em}}}{2\pi R}\Big[e^{-i(\phi-\xi)}\left(k - \frac{1}{2}\frac{d\chi^b}{d\ell} + \frac{1}{2}\frac{d\xi}{d\ell}\right)\frac{\sin\zeta}{2} + e^{i(\phi-\xi)}\left(k - \frac{1}{2}\frac{d\chi^b}{d\ell} - \frac{1}{2}\frac{d\xi}{d\ell}\right)\frac{\sin\zeta}{2} \\ &+ \frac{i}{2}\frac{d\zeta}{d\ell}\left(\sin^2\frac{\zeta}{2}e^{i(\phi-\xi)} - \cos^2\frac{\zeta}{2}e^{-i(\phi-\xi)}\right)\Big].\end{aligned} \tag{49}$$

The spin-orbit interaction energy density for the φ_k^a and φ_{-k}^b pair is thus given by

$$h_{so;k}^{\text{ring}} = \frac{\lambda E^{\text{em}}}{2\pi R}\left(e^{-i(\phi-\xi)} + e^{-i(\phi-\xi)}\right)\left(2k - \frac{1}{2}\frac{d(\chi^a - \chi^b)}{d\ell}\right)\frac{\sin\zeta}{2}. \tag{50}$$

In the following, we assume that $\frac{d\chi^a}{d\ell}$ and $\frac{d\chi^b}{d\ell}$ are constant. To make the magnitude of $h_{so;k}^{\text{ring}}$ large, we take $\zeta = \pi/2$; this means that the electron spin is lying in the x-y plane. We also choose $\xi = \phi$ to make $\left(e^{-i(\phi-\xi)} + e^{-i(\phi-\xi)}\right)$ in $h_{so;k}^{\text{ring}}$ constant along the ring. We denote φ_k^a and φ_k^b with the above-mentioned choices by $\bar{\varphi}_k^a$ and $\bar{\varphi}_k^b$.

The condition $\xi = \phi$ means that the direction of spin rotates when electrons move around the ring with $w_C[\xi] = 1$. Then, the conditions in Eq. (44) impose constraints

$$w_C[\chi^a] = \text{odd integer}; \quad w_C[\chi^b] = \text{odd integer}. \tag{51}$$

Non-zero current density appears according to Eq. (47), which is expected to be stable due to the topological protection by $w_C[\xi] = 1$, $w_C[\chi^a] = \text{odd}$, and $w_C[\chi^b] = \text{odd}$.

By employing $\bar{\varphi}^a_k$ and $\bar{\varphi}^b_k$, $h^{\rm ring}_{so;k}$ is calculated as

$$\bar{h}^{\rm ring}_{so;k} = \frac{\lambda E_{\rm em}}{2\pi R}\left(2k - \frac{1}{2}\frac{d(\chi^a - \chi^b)}{d\ell}\right). \tag{52}$$

The kinetic energy density for $\bar{\varphi}^t_k$, $(t = a, b)$, is calculated as

$$(\bar{\varphi}^t_k)^* H^{\rm ring}_0 \bar{\varphi}^t_k = \frac{1}{4\pi m^* R}\Big[k^2 + \frac{1}{4}\left(\frac{d\chi^t}{d\ell}\right)^2 + \frac{1}{4R^2} - k\frac{d\chi^t}{d\ell}\Big]. \tag{53}$$

The kinetic energy density for the $\bar{\varphi}^a_k$ and $\bar{\varphi}^b_{-k}$ pair is given by

$$h^{\rm ring}_{0;k} = \frac{1}{4\pi m^* R}\Big[2k^2 + \frac{1}{4}\left(\frac{d\chi^a}{d\ell}\right)^2 + \frac{1}{4}\left(\frac{d\chi^b}{d\ell}\right)^2 + \frac{1}{2R^2} - k\frac{d(\chi^a - \chi^b)}{d\ell}\Big]. \tag{54}$$

Using the creation operators $a^\dagger_k$ and $b^\dagger_{-k}$ for $\bar{\varphi}^a_k$ and $\bar{\varphi}^b_{-k}$, respectively, the BCS type state vector is expressed as

$$|\widetilde{\rm BCS}^{\rm ring}\rangle = \prod_k (u_k + v_k a^\dagger_k b^\dagger_{-k})|{\rm vac}\rangle. \tag{55}$$

Now we calculate the total energy for $|\widetilde{\rm BCS}^{\rm ring}\rangle$. The spin-orbit interaction energy is calculated as

$$E^{\rm ring}_{so} = \lambda E_{\rm em}\sum_k v_k^2\left(2k - \frac{1}{2}\frac{d(\chi^a - \chi^b)}{d\ell}\right) = -\frac{\lambda E_{\rm em} N}{4}\frac{d(\chi^a - \chi^b)}{d\ell} \tag{56}$$

and the kinetic energy is calculated as

$$\begin{aligned} E^{\rm ring}_0 &= \sum_k v_k^2 \frac{1}{2m^*}\Big[2k^2 + \frac{1}{4}\left(\frac{d\chi^a}{d\ell}\right)^2 + \frac{1}{4}\left(\frac{d\chi^b}{d\ell}\right)^2 + \frac{1}{2R^2} - k\frac{d(\chi^a - \chi^b)}{d\ell}\Big] \\ &= \sum_k v_k^2 \frac{k^2}{m^*} + \frac{N}{16m^*}\left[\left(\frac{d\chi^a}{d\ell}\right)^2 + \left(\frac{d\chi^b}{d\ell}\right)^2 + \frac{2}{R^2}\right], \end{aligned} \tag{57}$$

where $N = \sum_k 2v_k^2$ is used.

Assuming that the pairing interaction energy is unaffected by the modification of the pairing states, the total energy increase by the modification of the pairing states is calculated as

$$\Delta E^{\rm ring} = \frac{N}{16m^*}\left[\left(\frac{d\chi^a}{d\ell}\right)^2 + \left(\frac{d\chi^b}{d\ell}\right)^2 + \frac{2}{R^2}\right] - \frac{\lambda E_{\rm em} N}{4}\frac{d(\chi^a - \chi^b)}{d\ell}. \tag{58}$$

The minimum occurs at

$$\frac{d\chi^a}{d\ell} = -\frac{d\chi^b}{d\ell} = 2m^* \lambda E_{\rm em} \tag{59}$$

with the minimum value $\Delta E^{\rm ring}_{min} = \frac{N}{8m^* R^2} - \frac{1}{2} m^* N \lambda^2 (E_{\rm em})^2$. Thus, if the condition

$$R > (2m^* |\lambda E_{\rm em}|)^{-1} \tag{60}$$

is satisfied, $\Delta E^{\rm ring}_{min}$ becomes negative. This means that the modified pairing states becomes more stable than the original one, thus, the modified pairing would occur in the ground state.

Due to the condition in Eq. (59), the minimum energy state is currentless from Eq. (48). A current carrying state is generated when this condition is upset. The resulting current is a stable one protected by the topological requirements in Eq. (51). In this case, if we introduce χ through

$$\chi^a = \nu + \chi; \quad \chi^b = -\nu + \chi, \tag{61}$$

and substituting χ^a and χ^b in Eq. (42), the resulting wave function is given in the from of Eq. (1). This indicates that the supercurrent is generated by the spin-twisting itinerant motion of electrons by the addition of the Rashba spin-orbit interaction.

IV. CONCLUDING REMARKS

The present work indicates that the flux quantum $hc/2e$ and the Josephson frequency $2eV_0/h$ are consequence of the appearance of the phase variable that generates the gauge invariant effective vector $\mathbf{A}^{\rm eff}$ and scalar potential $\varphi^{\rm eff}$ given in Eqs. (10) and (12), respectively. It also suggests that although the BCS theory succeeded in explaining how $T_{\rm c}$ is determined in a class of superconductors (the *BCS superconductors*), its supercurrent generation mechanism may be incorrect. It may be generated by the spin-twisting itinerant motion of electrons.

In the BCS theory, the Meissner effect is explained using the current derived by the perturbation theory regarding $\mathbf{A}^{\rm em}$ as the perturbation [11]. On the other hand, the current is derived in a non-perturbative way in the new theory as in the Ginzburg-Landau theory. The latter current is gauge invariant, but the former is not. The restoration of the gauge invariance in the former is achieved by including the terms that violate the particle number conservation and the phase which violates the superselection rule for the charge [30, 31]. On the other hand, that the Meissner effect and related supercurrent phenomena are explained within the particle number fixed formalism. This is more in accordance with the fact that the number of particles in a superconductor is fixed. This will also allow to obtain the wave functions from the microscopic Hamiltonian by solving the Schrödinger equation.

The experimental facts indicate that the supercurrent carrying state is a stable or metastable state with an ability to adjust itself to different boundary conditions flexibly; the explanation for this property is lacking in the BCS theory. On the other hand, the metastability of the current carrying state is explained as due to the constraint of the topological winding number in Eq. (6) in the new theory; flexible adjustment to different boundary conditions can be attributed to the fact that the condition in Eq. (6) allows numerous different current patterns if the number of spin-vortices is large.

Although the major change occurs in the mechanism of the supercurrent generation in the new mechanism, the Ginzburg-Landau theory and the Josephson relations (Eqs. (13) and (14)) are unaffected. Subtle differences exist in the dependence of the maximum supercurrent flow through the Josephson junctions on the applied magnetic field [1]; the latter may be used to check the validity of the new theory.

[1] H. Koizumi, J. Supercond. Nov. Magn. **24**, 1997 (2011).

[2] R. Hidekata and H. Koizumi, J. Supercond. Nov. Magn. **24**, 2253 (2011).

[3] H. Koizumi, R. Hidekata, A. Okazaki, and M. Tachiki, J Supercond Nov Magn **27**, 121 (2014).

[4] H. Koizumi, A. Okazaki, M. Abou Ghantous, and M. Tachiki, J. Supercond. Nov. Magn. (DOI: 10.1007/s10948-014-2626-9).

[5] R. P. Feynman, R. Leighton, and M. sands, *Lectures on physics*, vol. 3 (Addison-wesley, Reading MA, 1965).

[6] N. W. Ashcroft and N. D. Mermin, *Solid State Physics* (Sauders College, Philadelphia PA, 1976).

[7] C. Kittel, *Introductio to Solid State Physics* (Wiley, USA, 1986), 6th ed.

[8] M. Tinkham, *Introduction to superconductivity* (MacGraw-Hill, USA, 1996), 2nd ed.

[9] H. K. Onnes, Leiden Comm. **119b** (1911).

[10] H. K. Onnes, Leiden Comm. **122b** (1911).

[11] J. Bardeen, L. N. Cooper, and J. R. Schrieffer, Phys. Rev. **108**, 1175 (1957).

[12] J. G. Bednorz and K. A. Müller, Z. Phys. **B64**, 189 (1986).

[13] V. J. Emery and S. A. Kivelson, Nature **374**, 434 (1995).

[14] H. C. Longuet-Higgins, U. Öpik, M. H. L. Pryce, and R. A. Sack, Proc. Roy. Soc. London Ser. A **244**, 1 (1958).

[15] E. Schrödinger, Ann. Physik **79**, 361 (1926).

[16] C. A. Mead and D. G. Truhlar, J. Chem. Phys. **70**, 2284 (1979).

[17] M. V. Berry, Proc. Roy. Soc. London Ser. A **391**, 45 (1984).

[18] E. I. Rashba, Sov. Phys. Solid State **2**, 1109 (1960).

[19] B. D. Josephson, Phys. Lett. **1**, 251 (1962).

[20] B. D. Josephson, Adv. Phys. **14**, 419 (1965).

[21] M. H. Cohen, L. M. Falicov, and J. C. Phillips, Phys. Rev. Lett. **8**, 316 (1962).

[22] P. W. Anderson and J. M. Rowell, Phys. Rev. Lett. **10**, 230 (1963).

[23] S. Shapiro, Phys. Rev. Lett. **11**, 80 (1963).

[24] C. C. Crimes and S. Shapiro, Phys. Rev. **169**, 397 (1968).

[25] M. D. Fiske, Rev. Mod. Phys. **36**, 221 (1963).

[26] I. K. Yanson, V. M. Svistunov, and I. M. Dmitrenko, J. Exptl. Theoret. Phys. (U.S.S.R.) **48**, 976 (1965).

[27] I. Giavever, Phys. Rev. Lett. **14**, 904 (1965).

[28] G. Rickayzen, *Theory of superconductivity* (Interscience, New York, 1965).

[29] J. R. Waldram, Rep. Prog. Phys. **39**, 751 (1976).

[30] P. W. Anderson, Phys. Rev. **112**, 1900 (1958).

[31] Y. Nambu, Phys. Rev. **117**, 648 (1960).